Continuous Spin Excitations in the Three-Dimensional Frustrated Magnet math xmlns="http://www.w3.org/1998/Math/MathML" display="inline">mrow>msub>mrow>mi mathvariant="normal">K/mi>/mrow>mrow>mn>2/mn>/mrow>/msub>msub>mrow>mi>Ni/mi>/mrow>mrow>mn>2/mn>/mrow>/msub>mo stretchy="false">(/mo>mrow>msub>mrow>mi>SO/mi>/mrow>mrow>mn>4/mn>/mrow>/msub>/mrow>msub>mrow>mo stretchy="false">)/mo>/mrow>mrow>mn>3/mn>/mrow>/msub>/mrow>/math>

Weiliang Yao, Qing Huang, Tao Xie, Andrey Podlesnyak, Alexander Brassington, Chengkun Xing, Ranuri S. Dissanayaka Mudiyanselage, Haozhe Wang, Weiwei Xie, Shengzhi Zhang, Minseong Lee, Vivien S. Zapf, Xiaojian Bai, D. Alan Tennant, Jian Liu, and Haidong Zhou

Phys. Rev. Lett. **131**, 146701 — Published 3 October 2023

DOI: 10.1103/PhysRevLett.131.146701

Continuous spin excitations in the three-dimensional frustrated magnet $K_2Ni_2(SO_4)_3$

Weiliang Yao,[1,*] Qing Huang,[1] Tao Xie,[2] Andrey Podlesnyak,[2] Alexander Brassington,[1] Chengkun Xing,[1] Ranuri S. Dissanayaka Mudiyanselage,[3] Haozhe Wang,[4] Weiwei Xie,[3,4] Shengzhi Zhang,[5] Minseong Lee,[5] Vivien S. Zapf,[5] Xiaojian Bai,[6] D. Alan Tennant,[1] Jian Liu,[1] and Haidong Zhou[1,†]

[1] *Department of Physics and Astronomy, University of Tennessee, Knoxville, TN 37996, USA*
[2] *Neutron Scattering Division, Oak Ridge National Laboratory, Oak Ridge, TN 37831, USA*
[3] *Department of Chemistry and Chemical Biology, Rutgers University, Piscataway, NJ 08854, USA*
[4] *Department of Chemistry, Michigan State University, East Lansing, MI 48824, USA*
[5] *National High Magnetic Field Laboratory, Los Alamos National Laboratory, Los Alamos, NM 87545, USA*
[6] *Department of Physics and Astronomy, Louisiana State University, Baton Rouge, LA 70803, USA*

(Dated: September 8, 2023)

Continuous spin excitations are widely recognized as one of the hallmarks of novel spin states in quantum magnets, such as quantum spin liquids (QSLs). Here, we report the observation of such kind of excitations in $K_2Ni_2(SO_4)_3$, which consists of two sets of intersected spin-1 (Ni^{2+}) trillium lattices. Our inelastic neutron scattering measurement on single crystals clearly shows a dominant excitation continuum, which exhibits a distinct temperature-dependent behavior from that of spin waves, and is rooted in strong quantum spin fluctuations. Further using the self-consistent-gaussian-approximation method, we determine that the fourth- and fifth-nearest neighbor exchange interactions are dominant. These two bonds together form a unique three-dimensional network of corner-sharing tetrahedra, which we name as "hyper-trillium" lattice. Our results provide direct evidence for the existence of QSL features in $K_2Ni_2(SO_4)_3$ and highlight the potential for the hyper-trillium lattice to host frustrated quantum magnetism.

For conventional insulating magnets, spins usually order at a finite temperature (*e.g.*, T_N), below which sharp spin waves emerge due to the propagation of spin fluctuations [1] (case I of Figure 1). When warming above the ordering temperature, spin waves disappear with paramagnetic fluctuations remaining. In contrast, quantum spin liquids (QSLs) have other spectroscopic features due to long-range quantum entanglement [2–5]. Namely, the spins can fractionalize into fermionic quasi-particles so that can only be detected in pairs by spectroscopic methods, which exhibit a continuous excitation spectrum [2–5] (case III of Fig. 1). For example, $Ce_2Zr_2O_7$ [6–9] and $NaCaNi_2F_7$ [10, 11] are two representative materials showing remarkable continuous spin excitations that are related to QSL. Due to the lacking of an ordering transition, the continuum transfers to paramagnetic spectrum through a crossover when warming up [12] (Fig. 1).

However, when geometric spin frustration and/or competing interactions are significant, some spin-ordered magnets will still exhibit remarkable QSL signatures including excitation continuum (case II of Fig. 1). The interplay of multiple ingredients suggests their magnetic properties may be susceptible to external tuning parameters, such as chemical doping [13], magnetic field [14], and pressure [15], which sets them apart from the above two categories. The Kitaev spin liquid candidate α-$RuCl_3$ has been studied as a celebrated example in the case II, which hosts both spin waves and continuous spin excitations in its antiferromagnetic ordered state [16–20]. On the one hand, a rod-like magnetic continuum at Brillouin zone center was observed by neutron, Raman, and terahertz spectroscopies [16–23], which has been widely viewed as a "smoking-gun" for fractionalized Majorana fermions. On the other hand, the long-range magnetic order and spin waves present at zero field can be fully suppressed by an in-plane magnetic field, resulting in a QSL state before partially magnetic polarization [19, 24–26].

More recently, the langbeinite compound $K_2Ni_2(SO_4)_3$

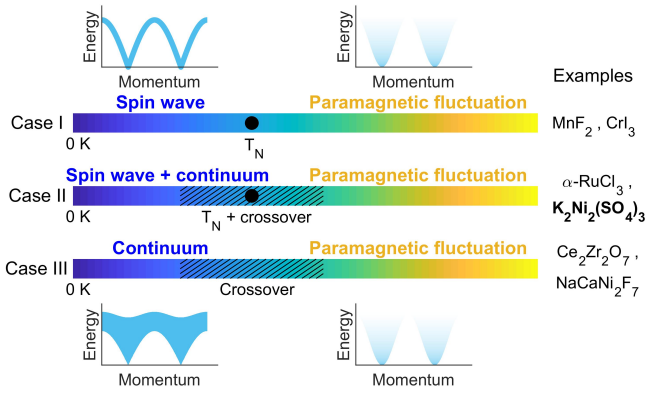

FIG. 1. Schematic of temperature-dependent behaviors for three types of spin excitations observed in magnetic materials with localized moments. Insets display the energy versus momentum relations. The black dots and hatched area denote the ordering temperature (*e.g.*, T_N) and crossover region, respectively. Representative materials of each case are listed on the right.

* weiliangyao@outlook.com; Present address: Department of Physics and Astronomy, Rice University, Houston, TX 77005, USA
† hzhou10@utk.edu

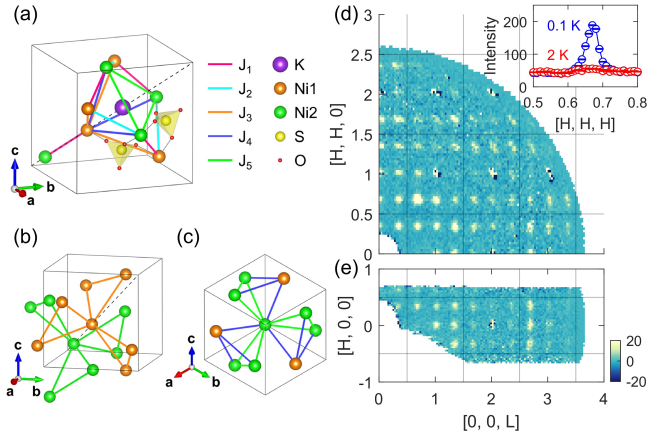

FIG. 2. (a) Crystal structure of $K_2Ni_2(SO_4)_3$. For clarity, only two SO_4^{2-} groups (depicted as yellow tetrahedra) and one K^+ ion are shown explicitly. Colored lines indicate exchange interactions of up to J_5 between Ni^{2+} ions. The dashed line represents the body diagonal along the [1, 1, 1] direction of the cubic unit cell. (b) Trillium lattices of Ni1 and Ni2 formed by J_3 and J_4 bonds, respectively. (c) Hyper-trillium lattice (see text) formed by J_4 and J_5 bonds. These structural illustrations were generated using VESTA [27]. (d) and (e) Magnetic diffraction patterns of the (H, H, L) and (H, 0, L) planes at 0.1 K, with the data at 2 K subtracted as background. The data in (d) are integrated over $[-0.05, 0.05]$ along $[K, -K, 0]$ and $[-0.05, 0.05]$ meV in energy. The data in (e) are integrated over $[-0.1, 0.1]$ along $[0, K, 0]$ and $[-0.05, 0.05]$ meV in energy. Solid lines represent Brillouin zone boundaries. The inset of (d) shows the intensity around (2/3, 2/3, 2/3) at 0.1 K and 2 K. The data are integrated over $[-0.05, 0.05]$ along $[K, -K, 0]$ and $[0.5L, 0.5L, -L]$, and $[-0.05, 0.05]$ meV in energy.

has been proposed to be another field-induced QSL based on thermodynamic and spectroscopic measurements [28]. With a cubic structure, $K_2Ni_2(SO_4)_3$ has two sets of spin-1 Ni^{2+}-trillium lattices interconnecting in three-dimensional (3D) space [Figure 2(a) and (b)] [28, 29]. Although magnetic phase transitions to spin-ordered states have been identified in this compound, prominent quantum spin fluctuations are evidenced by a broad hump in magnetic specific heat and a plateau of relaxation rate in muon spin spectroscopy (μSR) [28]. Appreciable magnetic diffuse scattering and continuum-like excitations were also respectively observed by neutron diffraction and inelastic neutron scattering (INS) on powder sample [28]. Moreover, a moderate magnetic field ~4 T can fully suppress the ordered spin components and drive the system into a QSL state [28]. These findings suggest that the magnetic order in $K_2Ni_2(SO_4)_3$ is fragile and it may approximate to a QSL at zero field. However, the nature of its spin dynamics is less clear due to the limitation of the powder data. In particular, whether the observed spin excitations are intrinsically continuous or simply powder-averaged spin waves is the major unknown.

In this work, we present an INS study on large and high-quality $K_2Ni_2(SO_4)_3$ single crystals. We find that although a long-range magnetic order develops below $T_N \approx 1.1$ K, its spin excitations are continuous even at temperatures well below T_N, such as down to 0.1 K. By studying these excitations over a temperature range covering almost three orders of magnitude, we conclude that they are distinct from spin-wave excitations observed in conventional magnets but similar to those continuous spin excitations in studied QSL candidates. With the self-consistent-gaussian-approximation (SCGA) method, we determine the fourth- and fifth-nearest-neighbor exchange interactions are dominant, which together construct a hitherto uncovered structure - the "hyper-trillium" lattice. Our study on $K_2Ni_2(SO_4)_3$ therefore shows another rare example for the existence of QSL features amid a spin-ordered state.

Single crystals of $K_2Ni_2(SO_4)_3$ were prepared with a self-flux method [28, 30]. In our INS experiment, 9 pieces of single crystals with a total mass of ~6 grams were cut and coaligned with the (H, H, L) plane being put in horizontal. The experiment was performed on the Cold Neutron Chopper Spectrometer (CNCS) installed at Spallation Neutron Source, Oak Ridge National Laboratory [37]. Throughout the experiment, an incident neutron energy of 3.32 meV was employed in the high flux mode. A dilution refrigerator insert was used to provide a base temperature of 0.1 K. We rotated the sample along the vertical [1, -1, 0] direction about 150° to fully cover one quadrant of the (H, H, L) plane. To present intensity maps of this plane, we symmetrized the data according to the crystal symmetry of $K_2Ni_2(SO_4)_3$. Four-dimensional INS data at six temperatures (0.1 K, 0.9 K, 2 K, 10 K, 20 K, and 80 K) were collected, which were reduced and analyzed with Horace [38]. The displayed neutron scattering intensity is proportional to the dynamic structure factor $S(\mathbf{Q}, E)$, which has been converted to absolute unit based on structural Bragg peaks as described in [30].

Fig. 2(d) and (e) show elastic magnetic scattering maps of the (H, H, L) and (H, 0, L) planes at 0.1 K. We can identify magnetic Bragg peaks at positions that are indexed by (1/3, 0, 0), (1/3, 1/3, 0), and (1/3, 1/3, 1/3), which is consistent with the previous report based on powder sample [28]. Additionally, we also find intensity at Brillouin zone centers [*e.g.*, at (0, 0, 1)], which might be caused by magnetic multiple scattering, or an extra magnetic wave vector $\mathbf{k} = (0, 0, 0)$. Despite the detailed magnetic structure is beyond this study, the coexistence of multiple propagation vectors indicates a magnetic ground state with several competing phases. We notice that two thermal phase transitions at 0.74 K and 1.14 K were reported previously [28]. However, we here only observe one transition at ~1.1 K by magnetic susceptibility and heat capacity measurements, and do not find a significant change of the magnetic Bragg peaks from 0.1 K to 0.9 K (see [30] for details). These observations support a unified magnetic phase in between, consistent with the constant relaxation rate in μSR [28].

Spin excitations at 0.1 K are presented in Figure 3. Albeit the temperature is only about $0.1T_N$, we find the

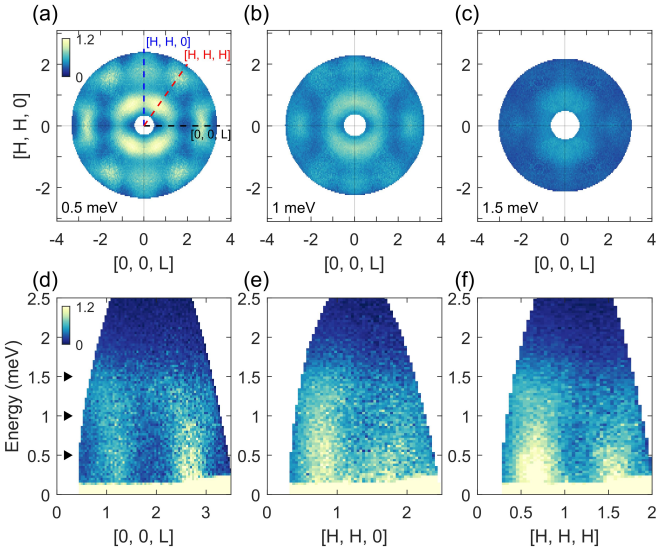

FIG. 3. (a)-(c) Constant-energy slices of the (H, H, L) plane at 0.1 K. The data are integrated over $[-0.1, 0.1]$ along $[K, -K, 0]$ and $[-0.1, 0.1]$ meV about specified energies. (d)-(f) Energy dependence of the magnetic continuum along high-symmetric directions [dashed lines in (a)]. The data in (d) are integrated over $[-0.05, 0.05]$ along $[H, H, 0]$ and $[K, -K, 0]$. The data in (e) are integrated over $[-0.05, 0.05]$ along $[0, 0, L]$ and $[K, -K, 0]$. The data in (f) are integrated over $[-0.05, 0.05]$ along $[K, -K, 0]$ and $[0.5L, 0.5L, -L]$. The right triangles in (d) indicate energy positions where the slices in (a)-(c) were taken.

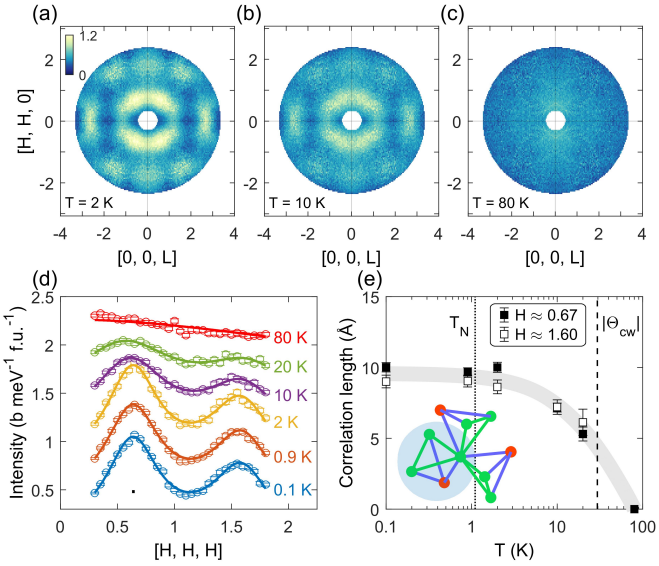

FIG. 4. (a)-(c) Constant-energy slices for 0.5 meV at 2 K, 10 K, and 80 K. The data are integrated over $[-0.1, 0.1]$ along $[K, -K, 0]$ and $[0.4, 0.6]$ meV in energy. (d) Momentum dependence of the intensity along $[H, H, H]$ obtained by integrating over E = [0.2, 1.0] meV and $[-0.05, 0.05]$ along $[K, -K, 0]$ and $[0.5L, 0.5L, -L]$. Data above 0.1 K are vertically offset for clarity. Solid curves are fits to the data as described in the text. Short horizontal bar indicates the momentum resolution. (e) Temperature dependence of the spin correlation length determined from the peak widths in (d). Bold grey line is a guide to the eyes. The dotted and dashed vertical lines mark the T_N and $|\Theta_{CW}|$, respectively. The inset shows the correlation sphere (shown in light blue) at 0.1 K with respect to tetrahedral units.

excitation spectrum is dominated by a broad continuum. The constant-energy slices in Fig. 3 (a)-(c) show that the dynamic structure factor reaches its maximum around (2/3, 2/3, 2/3) in the (H, H, L) plane, which corresponds to the strongest magnetic Bragg peak [Fig. 2(d)]. This indicates the continuous spin excitations are intimately related to the underlying magnetic order. According to energy–momentum slices [Fig. 3 (d)-(f)], these excitations are gapless and extend up to ∼2 meV, which is consistent with the Curie-Weiss temperature [Θ_{CW} = -29.6(1) K] [30] and the reported powder INS data [28].

Upon warming to 2 K, the scattering pattern is largely intact [Figure 4(a)], even though the long-range magnetic order has faded away [see the inset of Fig. 2(d)]. Similar scattering pattern is still apparent at 10 K [Fig. 4(b)], and finally becomes featureless at 80 K [Fig. 4(c)], where the intensity decays with the momentum transfer by following the magnetic form factor of Ni^{2+} [see Fig. 4(d) and [30]]. Energy–momentum slices at other five temperatures are presented in Fig. S10 of [30]. This temperature-dependent behavior further confirms that the observed signal is from magnetic scattering. By analyzing these temperature-dependent data, we estimate the spectral weight in the elastic channel is 8%∼20% of the total [30]. On the other hand, for a conventional spin-1 Heisenberg magnet, half of the spectral weight is expected to be elastic. The much enhanced dynamic spectral weight in $K_2Ni_2(SO_4)_3$ is indicative of strong quantum spin fluctuations at low temperature [11], which differs from the high-temperature region where thermal fluctuations dominate. Similar observation has been made on the QSL candidate $NaCaNi_2F_7$ [11], in which ∼90% of the neutron scattering spectral weight forms continuous spin excitations. Like a number of quantum materials with a magnetically ordered ground state [39–41], the static spin component of Ni^{2+} in $K_2Ni_2(SO_4)_3$ is greatly reduced by these quantum fluctuations.

In Fig. 4(d), we show constant-energy cuts (of E = [0.2, 1.0] meV) along $[H, H, H]$. At temperatures below 80 K, there are two broad peaks at $H \approx 0.67$ and $H \approx 1.60$, which can be well fitted by a double-Lorentzian profile multiplied with the square of magnetic form factor [solid curves in Fig. 4(d)]. Based on the fitted peak widths, we extracted the spin correlation lengths at various temperatures [42, 43], which are presented in Fig. 4(e). Since there is no peak can be resolved for the data at 80 K, we fit them only by the square of the magnetic form factor and set the correlation length to be zero. More details of the fitting and analysis can be found in [30]. We note that after being calibrated by the magnetic form factor, the intensities of the two peaks are basically

identical [30], reasonably consistent with the comparable spin correlation lengths deduced from them.

The spin correlation length at 0.1 K (ξ_0) is about 9.5 Å. It is much smaller than the one estimated based on the magnetic Bragg peak [inset of Fig. 2(d)], which is about 197 Å. The greatly reduced correlation length for the inelastic signal indicates its short-range nature. Interestingly, the correlation sphere defined by ξ_0 approximately covers the tetrahedral unit formed by Ni1 and Ni2 [inset of Fig. 4(e)], which will be discussed below. There are two noteworthy features in the temperature dependence of this correlation length. First, it is only below $\sim|\Theta_{\rm CW}|$ that the spin correlation significantly establishes, which reflects the fact that the exchange interactions govern the spin dynamics. Second and more importantly, it is basically unchanged when the temperature goes across T_N. This behavior is different from conventional spin waves, where the correlation length is expected to decrease on approaching the ordering temperature [44, 45]. Such insensitivity to the T_N reveals that the major spin dynamics of $K_2Ni_2(SO_4)_3$ is distinct from spin waves. Instead, the thermal evolution of the correlation length resembles those studied QSLs [46, 47], indicating the observed continuous spin excitations may originate from a QSL state.

Despite the excitation continuum is an important signature of a QSL state, other external factors especially structural disorder may also contribute to such behavior, which has plagued the studies of many QSL candidates [3, 48–51]. However, in our case, it is very unlikely that the excitation continuum originates from disorder. First, due to the different valences and ionic radii for K^+, Ni^{2+}, and SO_4^{2-}, site mixture is chemically not allowed in $K_2Ni_2(SO_4)_3$. Our X-ray diffraction studies have further confirmed that the crystals have a langbeinite structure (see [30]), which has long been established in a variety of materials [29, 52, 53]. Second, the clear magnetic Bragg peaks at low temperature are against a significant contribution from severe structural disorder, which otherwise often leads to a spin glass ground state without long-range magnetic order at all [51].

Next, we establish the major exchange interactions of $K_2Ni_2(SO_4)_3$ with the SCGA method, which has been widely used to determine magnetic exchange interactions in frustrated magnets [9, 11, 54–59]. In our calculation, we used the following isotropic Heisenberg Hamiltonian as a starting point

$$H = \frac{1}{2}\sum_{n=1}^{5} J_n \sum_{i,j} \mathbf{S}_i \cdot \mathbf{S}_j, \qquad (1)$$

where J_1, $\cdots$, J_5 are exchange interactions up to fifth-nearest-neighbor. Figure 5(a) shows the energy-integrated intensity map at 2 K, which is approximately proportional to the magnetic structure factor. By fitting this spectrum with the SCGA method, we determined the exchange interactions as J_1 = -0.03(2) meV; J_2 = 0.00(1) meV; J_3 = 0.01(1) meV; J_4 = 0.47(2) meV; J_5 = 0.26(2) meV. The details of the SCGA calculation can be found in [30]. With these parameters, the calculated intensity map is presented in Fig. 5(b), which reproduces most of the features in our data. We point out that a single-ion anisotropic term is usually allowed for $S = 1$ Ni^{2+} ions, yet in our case, the inclusion of it cannot significantly improve the fitting [30]. Therefore, this Hamiltonian can be regarded as a minimum effective model for the magnetism of $K_2Ni_2(SO_4)_3$.

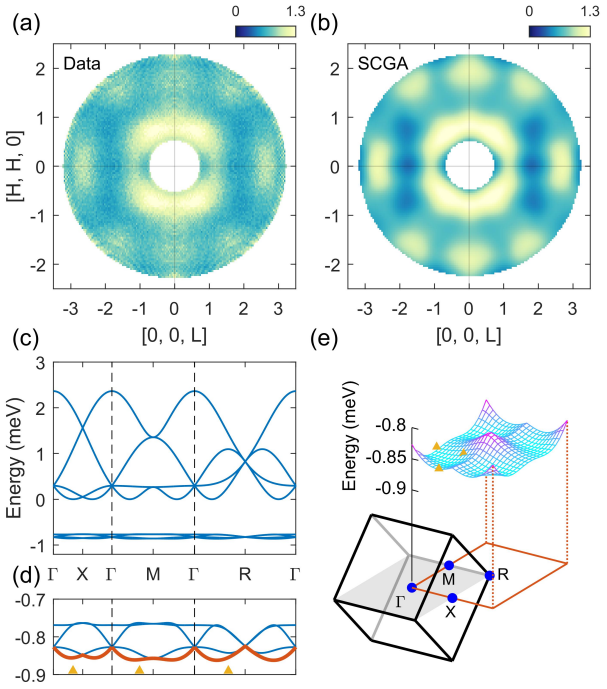

FIG. 5. (a) Energy-integrated intensity map (from 0.15 meV to 2 meV) of the (H, H, L) plane at 2 K. The momentum is integrated over $[-0.05, 0.05]$ along $[K, -K, 0]$. (b) The corresponding scattering pattern calculated using the SCGA method. (c) Dispersion curves for the interaction matrix along high-symmetric directions in the Brillouin zone. (d) A zoom-in view of four energy bands around -0.8 meV in (c). The energy band with the lowest energy is highlighted in orange. (e) The lowest energy band shown in the (H, H, L) plane. The cube is the first Brillouin zone, with high-symmetric points indicated by blue dots. The upper triangles in (d) and (e) indicate the positions of the three magnetic wave vectors observed experimentally.

To inspect the magnetic ground state, we further calculated the energy bands of the interaction matrix [30], where momentum positions with minimum energy predict the magnetic ordering wave vector in the mean-field level [60]. As presented in Fig. 5(c), there are four low-energy bands that are extremely flat, which naturally accounts for the highly frustrated nature of this system. Looking closer at these flat bands, we find the observed ordering wave vectors locate around the valley of the lowest-energy band [Fig. 5(d) and (e)]. It again suggests that the determined Hamiltonian is a good approximation, and the system features a variety of competing ordered states with very close energy. Through the "order-

by-disorder" mechanism [61–64], the quantum spin fluctuations may select particular spin patterns from these nearly degenerate classical ground states, which leads to the observed magnetic propagation wave vectors. Although the details of the development of long-range magnetic order can only be clarified after knowing the exact magnetic structure, it would be interesting to see how the magnetic order will be changed by tuning the magnitude of quantum fluctuations. A straightforward approach is to replace Ni^{2+} with other ions that have a different spin quantum number, such as Cu^{2+} with $S = 1/2$ and Co^{2+} with spin-orbital coupled $J_{\text{eff}} = 1/2$.

For this set of parameters, it is noteworthy that J_4 and J_5 are significant, and other exchange interactions are negligibly small. Structurally, the bonds of J_4 and J_5 together form a 3D lattice with corner-sharing tetrahedra [Fig. 2(c)], reminiscent of the pyrochlore lattice [65]. Due to the slight difference between the bond lengths of J_4 and J_5 (by ∼0.1 % [30]), Ni1 and Ni2 are fundamentally inequivalent in this 3D network. Specifically, three tetrahedra share one corner at the Ni2 site, while each Ni1 only belongs to one tetrahedron, which connects to Ni2 through J_4. To the best of our knowledge, such kind of lattice has never been reported before. In order to facilitate future studies on this newly identified structure, we here dub it as *hyper-trillium* lattice. Additional structural illustrations showing more tetrahedral units can be found in Fig. S3 of [30]. It is easy to see that the hyper-trillium lattice inherits the 3D connection from the trillium lattice [Fig. 2(b)]. The common magnetic propagation wave vector (1/3, 0, 0) for both the trillium lattice and $K_2Ni_2(SO_4)_3$ further hints their close relationship [66–69]. Nevertheless, our finding indicates the hyper-trillium lattice would be a more straightforward model to describe the magnetism of $K_2Ni_2(SO_4)_3$, rather than two sets of trillium lattices.

The prominence of J_4 and J_5 can be understood from the structural perspective. We first note that all Ni-Ni exchange interactions up to J_5 are mediated by the SO_4^{2-} group, which form a Ni-O-S-O-Ni super-superexchange path [Fig. 2(a)]. Farther interactions (J_6 ...) involve multiple intermediate groups, making them considerably weaker. For J_3, J_4, and J_5, their exchange paths (Ni-O-S-O-Ni) are more straight than those of J_1 and J_2, which can be more directly seen from the bond angle of Ni-S-Ni (see Table S3 in [30]). Moreover, the K^+ ion locates very closely to the center of the tetrahedral unit formed by J_4 and J_5 [Fig. 2(a)]. This cation may attract more electrons to hop around this region, so that enhance the exchange interaction. Therefore, the formation of the hyper-trillium lattice can be attributed to the combination of relatively straight exchange paths and cation attraction effect.

In summary, we have observed continuous spin excitations in $K_2Ni_2(SO_4)_3$ with INS, which persist well below its T_N. The temperature dependence of these excitations shows a distinct behavior from that of conventional spin waves, suggesting a close connection to QSL. Using the SCGA method, we have determined that the fourth- and fifth-nearest-neighbor exchange interactions are dominant, which effectively constitute a hyper-trillium lattice that is responsible for the much enhanced spin frustration. Our study not only uncovers decisive QSL features in $K_2Ni_2(SO_4)_3$, but also demonstrates that the hyper-trillium lattice is a new platform to explore frustrated quantum magnetism. As an immediate consequence, it may be applicable to a large number of other langbeinite compounds with rich chemical variants [29, 52, 53], which is expected to stimulate wide-ranging research of interest, as those pyrochlore oxides have done in the past few decades [65]. Ultimately, future studies aimed at clarifying the essence of the observed excitation continuum, *i.e.*, whether it is truly related to fractionalized fermionic excitations, are desirable.

Acknowledgments We wish to thank Tianran Chen, Tong Chen, Seung-Hwan Do, Chunruo Duan, Bin Gao, Dongliang Gong, Martin Mourigal, and Feng Ye for discussion. This research was supported by the U.S. Department of Energy under grant No. DE-SC0020254. This research used resources at the Spallation Neutron Source, a DOE Office of Science User Facility operated by the Oak Ridge National Laboratory. Part of the work was done in the National High Magnetic Field Laboratory, supported by the U.S. Department of Energy, Office of Science, National Quantum Information Sciences Research Centers, Quantum Science Center. The facilities of the National High Magnetic Field Laboratory are supported by the National Science Foundation Cooperative Agreement No. DMR-1644779, and the State of Florida and the U.S. Department of Energy. S. Z. also acknowledges LDRD program at Los Alamos National Laboratory.

[1] F. Bloch, Zeitschrift für Physik **61**, 206 (1930).
[2] L. Balents, Nature **464**, 199 (2010).
[3] J. Wen, S.-L. Yu, S. Li, W. Yu, and J.-X. Li, npj Quantum Materials **4**, 1 (2019).
[4] D. Wulferding, Y. Choi, W. Lee, and K.-Y. Choi, Journal of Physics: Condensed Matter **32**, 043001 (2019).
[5] J. Knolle and R. Moessner, Annual Review of Condensed Matter Physics **10**, 451 (2019).
[6] B. Gao, T. Chen, D. W. Tam, C.-L. Huang, K. Sasmal, D. T. Adroja, F. Ye, H. Cao, G. Sala, M. B. Stone, *et al.*, Nature Physics **15**, 1052 (2019).
[7] J. Gaudet, E. M. Smith, J. Dudemaine, J. Beare, C. R. C. Buhariwalla, N. P. Butch, M. B. Stone, A. I. Kolesnikov, G. Xu, D. R. Yahne, K. A. Ross, C. A. Marjerrison, J. D. Garrett, G. M. Luke, A. D. Bianchi, and B. D. Gaulin, Phys. Rev. Lett. **122**, 187201 (2019).

[8] E. M. Smith, O. Benton, D. R. Yahne, B. Placke, R. Schäfer, J. Gaudet, J. Dudemaine, A. Fitterman, J. Beare, A. R. Wildes, S. Bhattacharya, T. DeLazzer, C. R. C. Buhariwalla, N. P. Butch, R. Movshovich, J. D. Garrett, C. A. Marjerrison, J. P. Clancy, E. Kermarrec, G. M. Luke, A. D. Bianchi, K. A. Ross, and B. D. Gaulin, Phys. Rev. X **12**, 021015 (2022).

[9] B. Gao, T. Chen, H. Yan, C. Duan, C.-L. Huang, X. P. Yao, F. Ye, C. Balz, J. R. Stewart, K. Nakajima, S. Ohira-Kawamura, G. Xu, X. Xu, S.-W. Cheong, E. Morosan, A. H. Nevidomskyy, G. Chen, and P. Dai, Phys. Rev. B **106**, 094425 (2022).

[10] J. W. Krizan and R. J. Cava, Phys. Rev. B **92**, 014406 (2015).

[11] K. Plumb, H. J. Changlani, A. Scheie, S. Zhang, J. Krizan, J. Rodriguez-Rivera, Y. Qiu, B. Winn, R. Cava, and C. L. Broholm, Nature Physics **15**, 54 (2019).

[12] L. Savary and L. Balents, Reports on Progress in Physics **80**, 016502 (2016).

[13] A. Zunger and O. I. Malyi, Chemical Reviews **121**, 3031 (2021).

[14] Z. Ma, K. Ran, J. Wang, S. Bao, Z. Cai, S. Li, and J. Wen, Chinese Physics B **27**, 106101 (2018).

[15] T. Biesner and E. Uykur, Crystals **10** (2020).

[16] A. Banerjee, C. Bridges, J.-Q. Yan, A. Aczel, L. Li, M. Stone, G. Granroth, M. Lumsden, Y. Yiu, J. Knolle, *et al.*, Nature materials **15**, 733 (2016).

[17] A. Banerjee, J. Yan, J. Knolle, C. A. Bridges, M. B. Stone, M. D. Lumsden, D. G. Mandrus, D. A. Tennant, R. Moessner, and S. E. Nagler, Science **356**, 1055 (2017).

[18] S.-H. Do, S.-Y. Park, J. Yoshitake, J. Nasu, Y. Motome, Y. S. Kwon, D. Adroja, D. Voneshen, K. Kim, T.-H. Jang, J.-H. Park, K.-Y. Choi, and S. Ji, Nature Physics **13**, 1079 (2017).

[19] A. Banerjee, P. Lampen-Kelley, J. Knolle, C. Balz, A. A. Aczel, B. Winn, Y. Liu, D. Pajerowski, J. Yan, C. A. Bridges, A. T. Savici, B. C. Chakoumakos, M. D. Lumsden, D. A. Tennant, R. Moessner, D. G. Mandrus, and S. E. Nagler, npj Quantum Materials **3**, 8 (2018).

[20] J.-H. Han, S.-H. Do, K.-Y. Choi, S.-Y. Park, J.-Y. Kim, S. Ji, K.-S. Kim, and J.-H. Park, arXiv preprint arXiv:2203.13407 (2022).

[21] L. J. Sandilands, Y. Tian, K. W. Plumb, Y.-J. Kim, and K. S. Burch, Phys. Rev. Lett. **114**, 147201 (2015).

[22] D. Wulferding, Y. Choi, S.-H. Do, C. H. Lee, P. Lemmens, C. Faugeras, Y. Gallais, and K.-Y. Choi, Nature Communications **11**, 1 (2020).

[23] A. Little, L. Wu, P. Lampen-Kelley, A. Banerjee, S. Patankar, D. Rees, C. A. Bridges, J.-Q. Yan, D. Mandrus, S. E. Nagler, and J. Orenstein, Phys. Rev. Lett. **119**, 227201 (2017).

[24] J. A. Sears, Y. Zhao, Z. Xu, J. W. Lynn, and Y.-J. Kim, Phys. Rev. B **95**, 180411 (2017).

[25] S.-H. Baek, S.-H. Do, K.-Y. Choi, Y. S. Kwon, A. U. B. Wolter, S. Nishimoto, J. van den Brink, and B. Büchner, Phys. Rev. Lett. **119**, 037201 (2017).

[26] C. Balz, P. Lampen-Kelley, A. Banerjee, J. Yan, Z. Lu, X. Hu, S. M. Yadav, Y. Takano, Y. Liu, D. A. Tennant, M. D. Lumsden, D. Mandrus, and S. E. Nagler, Phys. Rev. B **100**, 060405 (2019).

[27] K. Momma and F. Izumi, Journal of Applied Crystallography **44**, 1272 (2011).

[28] I. Živković, V. Favre, C. Salazar Mejia, H. O. Jeschke, A. Magrez, B. Dabholkar, V. Noculak, R. S. Freitas, M. Jeong, N. G. Hegde, L. Testa, P. Babkevich, Y. Su, P. Manuel, H. Luetkens, C. Baines, P. J. Baker, J. Wosnitza, O. Zaharko, Y. Iqbal, J. Reuther, and H. M. Rønnow, Phys. Rev. Lett. **127**, 157204 (2021).

[29] D. Speer and E. Salje, Physics and Chemistry of Minerals **13**, 17 (1986).

[30] See Supplemental Material [url] for additional data and analyses, which includes Refs. [31–36].

[31] J. Rodríguez-Carvajal, Physica B: Condensed Matter **192**, 55 (1993).

[32] L. S. Wu, W. J. Gannon, I. A. Zaliznyak, A. M. Tsvelik, M. Brockmann, J.-S. Caux, M. S. Kim, Y. Qiu, J. R. D. Copley, G. Ehlers, A. Podlesnyak, and M. C. Aronson, Science **352**, 1206 (2016).

[33] G. G. Marcus, D.-J. Kim, J. A. Tutmaher, J. A. Rodriguez-Rivera, J. O. Birk, C. Niedermeyer, H. Lee, Z. Fisk, and C. L. Broholm, Phys. Rev. Lett. **120**, 097201 (2018).

[34] Y. Luo, G. G. Marcus, B. A. Trump, J. Kindervater, M. B. Stone, J. A. Rodriguez-Rivera, Y. Qiu, T. M. McQueen, O. Tchernyshyov, and C. Broholm, Phys. Rev. B **101**, 144411 (2020).

[35] G. Shirane, S. M. Shapiro, and J. M. Tranquada, *Neutron scattering with a triple-axis spectrometer: basic techniques* (Cambridge University Press, 2002).

[36] S. Toth and B. Lake, Journal of Physics: Condensed Matter **27**, 166002 (2015).

[37] G. Ehlers, A. A. Podlesnyak, J. L. Niedziela, E. B. Iverson, and P. E. Sokol, Review of Scientific Instruments **82**, 085108 (2011).

[38] R. Ewings, A. Buts, M. Le, J. Van Duijn, I. Bustinduy, and T. Perring, Nuclear Instruments and Methods in Physics Research Section A: Accelerators, Spectrometers, Detectors and Associated Equipment **834**, 132 (2016).

[39] A. Zheludev, M. Kenzelmann, S. Raymond, T. Masuda, K. Uchinokura, and S.-H. Lee, Phys. Rev. B **65**, 014402 (2001).

[40] B. Lake, D. A. Tennant, C. D. Frost, and S. E. Nagler, Nature Materials **4**, 329 (2005).

[41] H. B. Cao, A. Banerjee, J.-Q. Yan, C. A. Bridges, M. D. Lumsden, D. G. Mandrus, D. A. Tennant, B. C. Chakoumakos, and S. E. Nagler, Phys. Rev. B **93**, 134423 (2016).

[42] G. J. MacDougall, D. Gout, J. L. Zarestky, G. Ehlers, A. Podlesnyak, M. A. McGuire, D. Mandrus, and S. E. Nagler, Proceedings of the National Academy of Sciences **108**, 15693 (2011).

[43] O. Young, A. R. Wildes, P. Manuel, B. Ouladdiaf, D. D. Khalyavin, G. Balakrishnan, and O. A. Petrenko, Phys. Rev. B **88**, 024411 (2013).

[44] J. W. Lynn, Phys. Rev. B **11**, 2624 (1975).

[45] J. W. Lynn and H. A. Mook, Phys. Rev. B **23**, 198 (1981).

[46] G. Xu, C. Broholm, Y.-A. Soh, G. Aeppli, J. F. DiTusa, Y. Chen, M. Kenzelmann, C. D. Frost, T. Ito, K. Oka, and H. Takagi, Science **317**, 1049 (2007).

[47] L. Clark, G. Sala, D. D. Maharaj, M. B. Stone, K. S. Knight, M. T. Telling, X. Wang, X. Xu, J. Kim, Y. Li, S.-W. Cheong, and B. D. Gaulin, Nature Physics **15**, 262 (2019).

[48] T.-H. Han, J. S. Helton, S. Chu, D. G. Nocera, J. A. Rodriguez-Rivera, C. Broholm, and Y. S. Lee, Nature **492**, 406 (2012).

[49] Y. Shen, Y.-D. Li, H. Wo, Y. Li, S. Shen, B. Pan,

Q. Wang, H. Walker, P. Steffens, M. Boehm, Y. Hao, D. Quintero-Castro, L. Harriger, M. Frontzek, L. Hao, S. Meng, Q. Zhang, G. Chen, and J. Zhao, Nature **540**, 559 (2016).
[50] J. A. Paddison, M. Daum, Z. Dun, G. Ehlers, Y. Liu, M. B. Stone, H. Zhou, and M. Mourigal, Nature Physics **13**, 117 (2017).
[51] Z. Ma, J. Wang, Z.-Y. Dong, J. Zhang, S. Li, S.-H. Zheng, Y. Yu, W. Wang, L. Che, K. Ran, S. Bao, Z. Cai, P. Čermák, A. Schneidewind, S. Yano, J. S. Gardner, X. Lu, S.-L. Yu, J.-M. Liu, S. Li, J.-X. Li, and J. Wen, Phys. Rev. Lett. **120**, 087201 (2018).
[52] G. Gattow and J. Zemann, Zeitschrift für anorganische und allgemeine Chemie **293**, 233 (1958).
[53] H. McMurdie, M. Morris, J. DeGroot, and H. Swanson, Journal of Research of the National Bureau of Standards. Section A, Physics and Chemistry **75**, 435 (1971).
[54] P. H. Conlon and J. T. Chalker, Phys. Rev. B **81**, 224413 (2010).
[55] O. Benton and N. Shannon, Journal of the Physical Society of Japan **84**, 104710 (2015).
[56] X. Bai, J. A. M. Paddison, E. Kapit, S. M. Koohpayeh, J.-J. Wen, S. E. Dutton, A. T. Savici, A. I. Kolesnikov, G. E. Granroth, C. L. Broholm, J. T. Chalker, and M. Mourigal, Phys. Rev. Lett. **122**, 097201 (2019).
[57] J. A. M. Paddison, Phys. Rev. Lett. **125**, 247202 (2020).
[58] Y. Gu, Q. Wang, H. Wo, Z. He, H. C. Walker, J. T. Park, M. Enderle, A. D. Christianson, W. Wang, and J. Zhao, Phys. Rev. B **106**, L060504 (2022).
[59] S. Gao, M. A. McGuire, Y. Liu, D. L. Abernathy, C. d. Cruz, M. Frontzek, M. B. Stone, and A. D. Christianson, Phys. Rev. Lett. **128**, 227201 (2022).
[60] J. N. Reimers, A. J. Berlinsky, and A.-C. Shi, Phys. Rev. B **43**, 865 (1991).
[61] J. Villain, R. Bidaux, J.-P. Carton, and R. Conte, Journal de Physique **41**, 1263 (1980).
[62] A. Chubukov, Phys. Rev. Lett. **69**, 832 (1992).
[63] D. Bergman, J. Alicea, E. Gull, S. Trebst, and L. Balents, Nature Physics **3**, 487 (2007).
[64] L. Savary, K. A. Ross, B. D. Gaulin, J. P. C. Ruff, and L. Balents, Phys. Rev. Lett. **109**, 167201 (2012).
[65] J. S. Gardner, M. J. P. Gingras, and J. E. Greedan, Rev. Mod. Phys. **82**, 53 (2010).
[66] J. M. Hopkinson and H.-Y. Kee, Phys. Rev. B **74**, 224441 (2006).
[67] J. M. Hopkinson and H.-Y. Kee, Phys. Rev. B **75**, 064430 (2007).
[68] S. V. Isakov, J. M. Hopkinson, and H.-Y. Kee, Phys. Rev. B **78**, 014404 (2008).
[69] J. M. Bulled, J. A. M. Paddison, A. Wildes, E. Lhotel, S. J. Cassidy, B. Pato-Doldán, L. C. Gómez-Aguirre, P. J. Saines, and A. L. Goodwin, Phys. Rev. Lett. **128**, 177201 (2022).